FABRICATION OF HOLLOW SILICA NANORODS USING NANOCRYSTALLINE CELLULOSE AS TEMPLATES

Guangshuai Fu,[a] Aijian He,[a] Yongcan Jin,[a] Qiang Cheng,[b] and Junlong Song[a,] *

A simple approach to fabricate hollow silica nanorods is reported, using nanocrystalline cellulose (NCC) as templates. Uniform NCC with the length of *ca*. 100 nm and a diameter of *ca*. 10 nm were prepared by hydrolysis of microcrystalline cellulose (MCC) in strong sulfuric acid condition. NCC was used as a template to prepare a core-shell composite of silica and NCC. The sol-gel reaction of tetraethyl orthosilicate (TEOS) was employed to coat NCC with a nano thickness of silica in the presence of ammonia. Finally, hollow silica nanorods were obtained by calcination of the composite at 600°C to remove the organic cellulose template completely. The obtained hollow silica nanorods were found to have uniform size and shape: with a length of *ca*. 100 nm, an inner diameter close to the original diameter of NCC, and a thickness of around 10 to 15 nm. These results suggest that NCC is an excellent template for manufacturing nano hollow materials with uniform shape and size.

Keywords: Hollow silica nanorods; Template; Sol–gel method; MCC; NCC

*Contact information: a: Jiangsu Provincial Key Lab of Pulp and Paper Science and Technology, Nanjing Forestry University, Nanjing, Jiangsu, 210037 P.R. China; b: Research Institute of Wood Industry, Chinese Academy of Forestry, Beijing, 100091 P.R. China; *Corresponding author: junlong.song@gmail.com*

INTRODUCTION

In recent years, considerable effort has been devoted to the design and controlled fabrication of nano-structured materials with functional properties (Caruso 2001). Hollow materials have attracted great interest due to their wide range of applications in drug delivery, catalysts supports, fuel cell, enzyme carrier, fluorescers, and so on (Chen *et al*. 2004; Xiao *et al*. 2006; Guo and Cui 2009; Scheel *et al*. 2009). Templating is the most used method to fabricate hollow materials. Templates used include soft templates (such as emulsion droplets, micelles, *etc*. (Caruso *et al*. 1998)), and hard templates (for example, polystyrene microspheres (Kato *et al*. 2010), calcium carbonate (Zhao *et al*. 2010), and gold particles (Obare *et al.* 2001), *etc.*). However, these templates are mostly used to prepare hollow spherical nanoparticles and are, most of the time, in the scale of micro size. So far, limited reports on fabrication of hollow nano, rod-like materials or other shapes are available (Zollfrank *et al*. 2007).

Recently, long hollow inorganic nanoparticle nanotubes have been fabricated by templating of electrospun block copolymer fibers with clay mineral platelets followed by interlinking of the platelets using condensation reactions. Finally the polymer template is removed by heat or UV/ozone treatment (Ras *et al*. 2007). Inorganic nanoparticles with hollow interiors were also constructed by coating self-assembled polymeric nano-objects with a thin Al_2O_3 layer, followed by removal of the polymer template upon heating (Ras *et al*. 2007).

Cellulose is capable of serving as a template for nanotube and nanorod materials. Cellulose is the most abundant and biodegradable natural polymer material on the planet. During its biosynthesis, it is expressed from enzyme rosettes in the form of 3 to 5 nm diameter fibrils that aggregate into larger microfibrils up to 20 nm in diameter (Lucia and Hubbe 2008). Therefore cellulose or fiber can be separated into nanoscale architectures, namely nanocrystalline cellulose (NCC), nanofibrils, and nanoscale cell wall architectures. Recently, NCC and nanofibrils have become widely considered for use in the reinforcement of plastics (Kim *et al.* 2009; Zoppe *et al*. 2009; Pei *et al.* 2011; Zhou *et al*. 2011).

NCC, the crystalline segments of elementary nanofibril crystalline cellulose fibrils after the amorphous segments have been removed, are usually obtained via treatment with strong acids at elevated temperature or with enzyme treatments. NCC is in the range of 100 to 300 nm long with diameters of several to tens nanometers (Bondeson *et al.* 2006; Morán *et al.* 2008; Lucia and Rojas 2009).

However, with respect to its size and shape, NCC can serve as a type of ideal template for nanotube and nanorod materials. Zollfrank and coworkers (2007) first successfully fabricated silica nanotubes with diameters of 10 to 30 nm, inner core diameters of approximately 3 nm, and lengths of up to 500 nm, using NCC as a template. In their procedures, oligopropylamino side chain was introduced onto the surface of NCC in the medium of dimethylsulfoxide (DMSO). Then the sol-gel process of tetraethyl orthosilicate (TEOS) was performed to deposit silica on the surface of NCC in aqueous solution. The oligopropylamino side chain is capable of catalyzing the formation of a silica layer, and therefore is responsible for the control of biosilica deposition in diatoms into the cellulose biopolymer.

In this article, we report a simple approach to fabricate silica nanorods using negatively charged NCC as template. When sulfuric acid is used as the hydrolyzing agent, it also chemically reacts with the surface hydroxyl groups of NCC to yield negatively charged (surface) sulfate groups (Lucia *et al.* 2010). In this investigation, we took advantage of the negatively charged property of NCC and employed the cationic surfactant cetyltrimethylammonium bromide (CTAB) to convert the surface charge of NCC to positive to promote deposition of silicic acid sol. Then, the polycondensation reaction of TEOS exclusively took place at the particles' surfaces in the presence of ammonia, following the so-called Stober process (Stöber *et al*. 1968). As a consequence, silica-coated NCC particles were successfully prepared. Hollow silica nanorods were finally obtained after calcination of the obtained composite of silica/NCC at 600°C for 6 hours to remove the organic template. The obtained hollow silica nanorods have uniform shape and size. They do not agglomerate or collapse after calcination. Hollow silica nanorods may have potential applications in controlled release capsules for drugs, dyes, inks, artificial cells, and fillers because of their lower density, large specific surface area, and optical properties.

EXPERIMENTAL

Materials

Microcrystalline cellulose (MCC) was obtained from Whatman (DP approx. 172). All other chemicals, including sulphuric acid (H_2SO_4, 95 to 98%), tetraethoxysilane (TEOS, >95%), cetyltrimethylammonium bromide (CTAB, 98%), aqueous ammonia (25% w/w), and ethanol (EtOH, >99.7%), were purchased from Everbright Chemical Inc. (Jiangsu, China). All chemicals were used as received without further purification. All solutions were prepared using distilled/deionized water, which was treated with a Milli-Q system (Millipore Corporation, US).

Preparation of Nanocrystalline Cellulose

The procedure of preparation of nanocrystalline cellulose (NCC) was adopted from Beck-Candanedo's method (Beck-Candanedo *et al*. 2005). NCC was obtained as follows: MCC (5 g) and H_2SO_4 (250 mL, 64 wt%) were charged into a 500-mL three-neck flask equipped with a mechanical stirrer. This mixture was hydrolyzed at 45°C for 30 min under a constant stirring rate of 300 rpm. Immediately following hydrolysis, suspensions were diluted 10-fold to stop the reaction. The suspensions were then centrifuged for 20 min at 12000 rpm, washed once with water, and recentrifuged. The procedure was repeated at least three times, or until the supernatant became turbid, to ensure the removal of excess acid. The suspension, at last, was transferred to a dialysis membrane bag with a molecular weight cutoff of 14,000, and dialyzed against water for several days until the water pH remained constant.

Synthesis of Composite of Silica/NCC

A typical coating process was performed as follows: 0.12g CTAB was dissolved in a mixture of 40 mL of H_2O, 20 mL of EtOH, 0.4 mL of aqueous ammonia, and 4 mL of NCC dispersion (0.5%w/v). These chemicals were put into a 250-mL three-neck flask, and the dispersion was stirred by a magnetic stirrer (250 rpm) for 10 min at 30°C. Then, 200 μL of TEOS was charged into the system, leading to a sol-gel reaction. TEOS was slowly added into the NCC+CTAB+NH_3 dispersion with stirring at 250 rpm at 30°C for 2 hours to allow the hydrolysis and condensation of TEOS and the formation of the silica/NCC composite. After the reaction, the NCC particles coated by the silica were separated from the excess chemicals and byproducts (silica particles) by centrifugation. Only the coated NCC particles were sedimented, and the supernatant was removed. Subsequently, pure water was added, and the sediment was redispersed. This separation procedure was repeated three times to remove most of the excess chemicals and byproducts. The resultant sediment (complex of silica/NCC) was obtained. The powder of complex of silica/NCC was obtained by drying at 50°C under vacuum for hours.

Fabrication of Hollow Silica Nanorods

The powder of silica/NCC composite was calcined at 600°C for 6 hours using a muffle furnace to remove the organic NCC core. Organic NCC was burned and released as CO_2 and water. Silica mineral was retained, and kept the shape under which it had been formed. As a consequence, hollow silica nanorods were finally obtained.

Characterizations

FTIR spectra of NCC, silica-coated NCC, and hollow silica nanorods were obtained with a Nicolet 210 spectrometer. The sample for FTIR analysis was dispersed in KBr and then powdered in a mortar. Approximately 1 mg of the obtained samples was mixed with about 200 mg KBr to obtain the required discs. Both specimens and KBr were carefully dried before disk preparation and were subjected to FTIR analysis immediately afterwards.

A TGA analyzer investigated the thermal stability of the composite of silica/NCC. TGA analysis was performed in N_2 from room temperature to 600°C at a heating rate of 20°C min^{-1}.

XRD measurements were performed to check the crystallinity of MCC, NCC, silica-coated NCC, and hollow silica nanorods. The diffracted intensity of Cu Kα radiation (k = 0.1542 nm; 50 kV, and 40 mA) was measured in a 2θ range between 10° and 45° for MCC and NCC at a speed of $0.05°\cdot s^{-1}$. In the case of silica-coated NCC and hollow silica nanorods, the corresponding values were 5° to 55° and $0.02°\cdot s^{-1}$.

The specific surface area was measured by the BET method for silica-coated NCC and hollow silica nanorods. The degassing temperature was 80°C, and the time was 12 hours.

The diameter and morphology of the particles were examined by transmission electron microscopy (TEM) (JEOL JEM-1011) at an accelerator voltage of 100 kV. To prepare the TEM specimens, the NCC, silica-coated NCC, and hollow silica nanorods were dispersed in absolute ethanol with ultrasonication for 10 min. And then one drop of suspension was dropped on a copper TEM grid with carbon membrane, and the NCC was stained by phosphotungstic acid. Excess water was blotted with a piece of filter paper.

RESULTS AND DISCUSSION

Preparation of Nanocrystalline Cellulose

Nanocrystalline cellulose (NCC) was obtained through hydrolysis of MCC with strong sulfuric acid. The procedure has been addressed in detail elsewhere (Beck-Candanedo *et al.* 2005). NCC obtained from sulfuric acid hydrolysis was dispersed well in water due to the negative surface charge of NCC, which originated from the reaction of sulfuric acid with the surface hydroxyl groups of NCC. NCC solution was very stable, and no precipitate was observed even after months of storage time. The TEM image of obtained NCC is shown in Fig. 1(a). The image shows that cellulose crystals have uniform shape with a length between 100 and 150 nm and a width about 10 nm.

The infrared (IR) spectrum of NCC is presented in Fig. 1(b) with the comparison of MCC. It can be seen that the IR spectra of MCC and NCC were very similar. The observed strong IR absorption bands at 3300, 2920, 1750, and 1100 cm^{-1} agree with the cellulose standard. The crystallinity of cellulose can be checked with the FTIR method based on Nelson and O’Connor’s procedures (Nelson and O'Connor 1964a,b). Their theory claims that the strength of peaks at a1429/a893 and a1372/a2900 have relationships with the crystallinity of cellulose, and therefore these two relative strength values can be regarded as two crystallinity indexes of cellulose. Another report compared these two indexes with the crystallinity index checked by XRD and obtained two regressed equations (China National Pulp and Paper Research Institute and Beijing Chemical Plant 1981). According to these two equations, the crystallinity indexes checked by FTIR for MCC and NCC were 0.78 and 0.86, respectively. This indicates that the crystallinity of NCC increased to some extent compared with MCC, which was caused by the removal of amorphous regions of cellulose by hydrolysis. The same effect was also supported by XRD results in Fig. 1(c), where stronger peaks can be observed for NCC. There are three peaks at 14°, 16°, and 22°, respectively, of which 22° is maximum, in agreement with the typical XRD pattern of cellulose I.

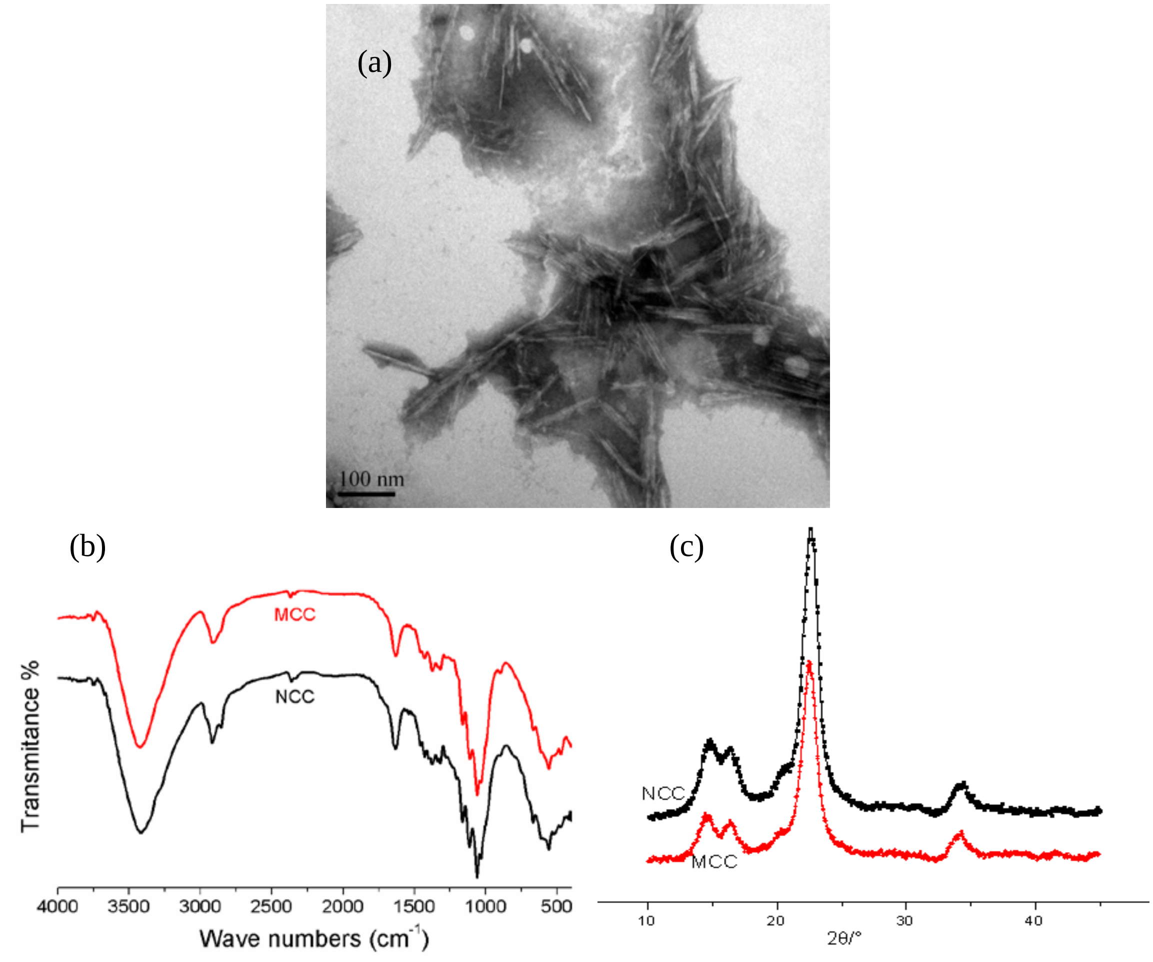

Fig. 1. (a) TEM image of nanocrystalline cellulose; (b) FTIR spectra of microcrystalline cellulose and nanocrystalline cellulose; (c) XRD of microcrystalline cellulose and nanocrystalline cellulose

Preparation of Silica-Coated NCC

A sol-gel process was employed to coat the NCC with a layer of silica. The sol-gel process is a wet-chemical technique widely used in the fields of materials science. Such methods are used primarily for the fabrication of materials (typically metal oxides) starting from a colloidal solution (sol) that acts as the precursor for an integrated network (or gel) of either discrete particles or network polymers (Min *et al.* 2009).

The sol–gel reactions of alkylsilane are as follows:
Alkylsilane hydrolysis in acid or basic conditions:

$$\text{Si-(OC}_2\text{H}_5)_4 + 4\text{H}_2\text{O} \rightarrow \text{Si-(OH)}_4 + 4\text{C}_2\text{H}_5\text{OH} \qquad (1)$$

Alcohol condensation:

$$\text{Si-(OH)}_4 + \text{Si-(OC}_2\text{H}_5)_4 \rightarrow \equiv\text{Si-O-Si}\equiv + 4\text{C}_2\text{H}_5\text{OH} \qquad (2)$$

Water condensation:

$$\text{Si-(OH)}_4 + \text{Si-(OH)}_4 \rightarrow \equiv\text{Si-O-Si}\equiv + 4\text{H}_2\text{O} \qquad (3)$$

In our case, NCC carried some negative charges, since MCC became hydrolyzed in the sulfuric acids, and etherification may occur between sulfuric acid and the surface hydroxyl groups of NCC (Lucia *et al.* 2010). Therefore, CTAB, a cationic polymer, was applied to the system to convert the surface charge of NCC to positive. Alkylsilane was initially hydrolyzed in the presence of ammonia to form silicic acid. Then, the formed silicic acid adsorbed onto the surface of NCC due to electrostatic attraction. Condensation with another alkylsilane or with itself to form cross-linked polysiloxane network was the last step. Therefore, a gel was formed and a composite of silica/NCC was prepared.

The TEM image of silica/NCC composite is presented in Fig. 2(a). It shows that these particles were very uniform as NCC, with the length of around 100 to 150 nm, but with an enlarged diameter about 30 to 40 nm, indicating that the silica layer was successfully coated onto the surface of NCC, and the thickness was about 10 to 15 nm. But it shows that these particles were agglomerated to some extent, similar to NCC.

The spectrum of the silica-coated NCC is shown in Fig. 3. The observed strong IR absorption bands at 1077 cm^{-1}, 470 cm^{-1} (Si–O–Si), and 800 cm^{-1} (Si-OH) indicate that the condensation reaction of TEOS took place at the particle surfaces. Sharp bands at 2924 cm^{-1} and 2853 cm^{-1} indicate the presence of an organic cellulose core.

Fabrication of Hollow Silica Nanorods

The cellulose core was removed from the composite particles by calcination. The TEM image of hollow silica nanorods is shown in Fig. 2(b), which clearly shows that the silica nanorods were hollow. The inner diameter of hollow silica nanorods was measured to be about 10 nm, which is close to the diameter of NCC. The outer diameter of nanorods was in the range of 30 to 40 nm, which agrees with the diameter of core-shell structured silica-coated NCC. This also reveals that the silica layer outside of NCC can preserve its shape even after removal of the core cellulose crystal template in the course of calcination. Moreover, these hollow silica nanoparticles do not collapse, but agglomerate to some extent.

The spectrum of hollow silica nanorods is presented in Fig. 3 along with the spectra of NCC and silica-coated NCC. From comparison, the characteristic IR absorption bands of hollow silica nanorods at 1077 cm^{-1}, 470 cm^{-1} (Si–O–Si), and 800 cm^{-1} (Si-OH) are more pronounced than those of silica-coated NCC, which indicates the

Fu *et al*. (2012). "Hollow SiO_2 nanorods from NCC," ***BioResources*** 7(2), 2319-2329. 2324

polymerization of polysiloxane and more cross-linked Si–O–Si bonds formed at elevated temperatures in the case of calcination. Sharp bands of silica-coated NCC at 2924 cm^{-1} and 2853 cm^{-1} totally disappeared this time, indicating that the organic cellulose core was completely removed due to calcination.

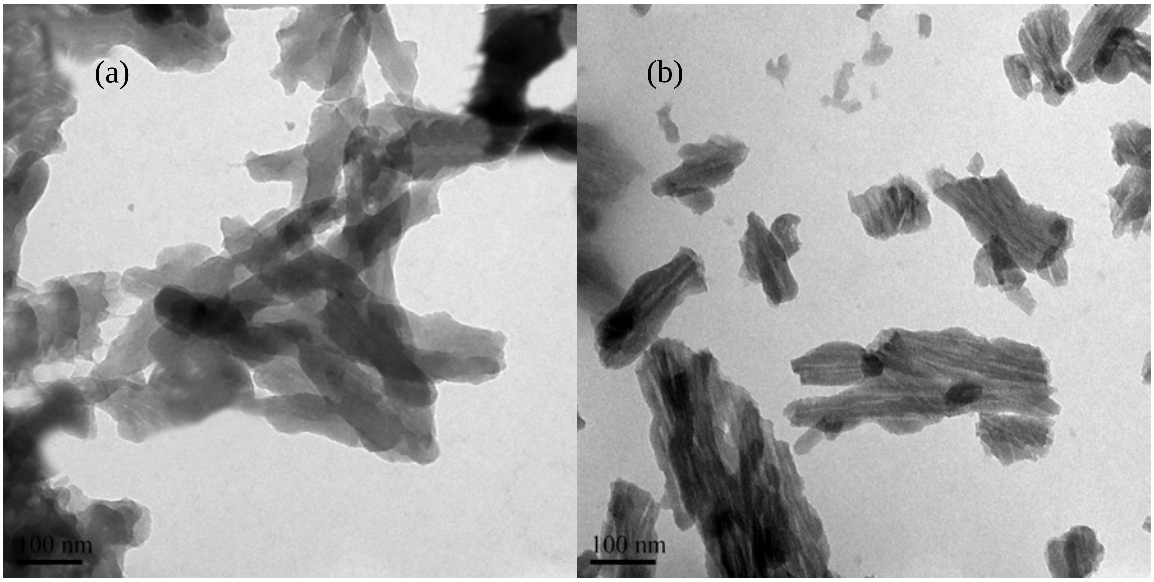

Fig. 2. TEM image of (a) silica-coated nanocrystalline cellulose and (b) hollow silica nanorods

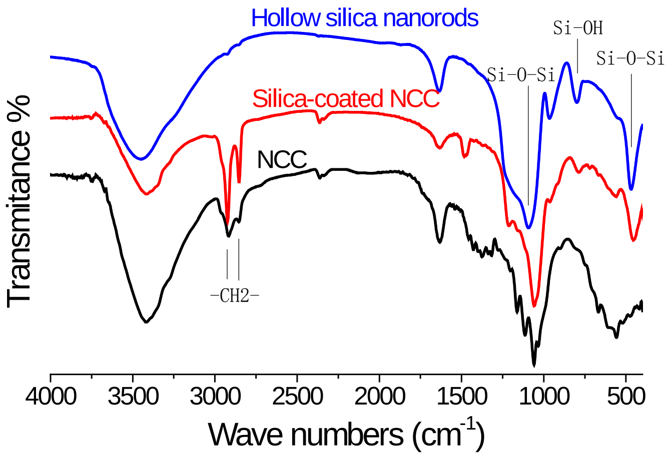

Fig. 3. FTIR spectra of nanocrystalline cellulose, silica-coated nanocrystalline cellulose, and hollow silica nanorods

The thermal stability of MCC, NCC, silica-coated NCC, and hollow silica nanorods is presented in Fig. 4. The thermal stability was measured by weight loss, as examined by TGA. The thermal decomposition temperature of NCC started from 250°C. Fast decomposition took place when the temperature was within the range of 250°C to 350°C. Since the reaction occurred in a nitrogen atmosphere, there was 20 percent residual carbon. The TGA curve of MCC was very close with that of NCC except with a higher residual carbon. After coating with silica, the thermal stability of NCC was significantly improved. Silica-coated NCC started to decompose at 250°C, and the weight remained constant after 400°C. However, a slight loss of weight can also be observed if one zooms the image to a larger scale. This can be attributed to the further condensation of Si-OH with the release of some small molecules. The TGA curve of hollow silica nanorods is the most stable one among all the TGA curves, and it exhibits almost a horizontal line in the graph.

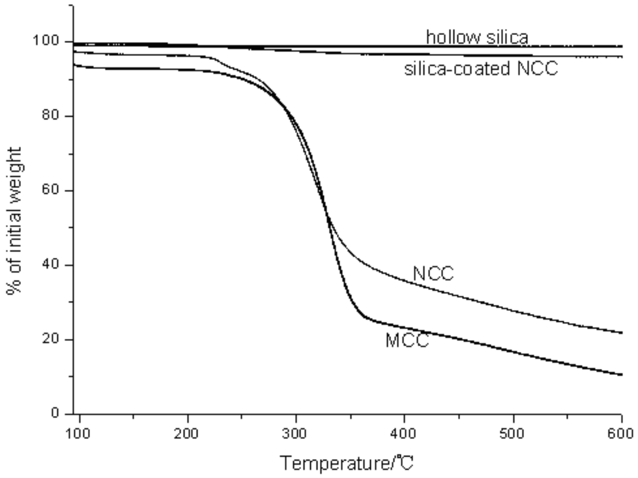

Fig. 4. Weight loss of microcrystalline cellulose, nanocrystalline cellulose, silica-coated nanocrystalline cellulose, and hollow silica nanorods

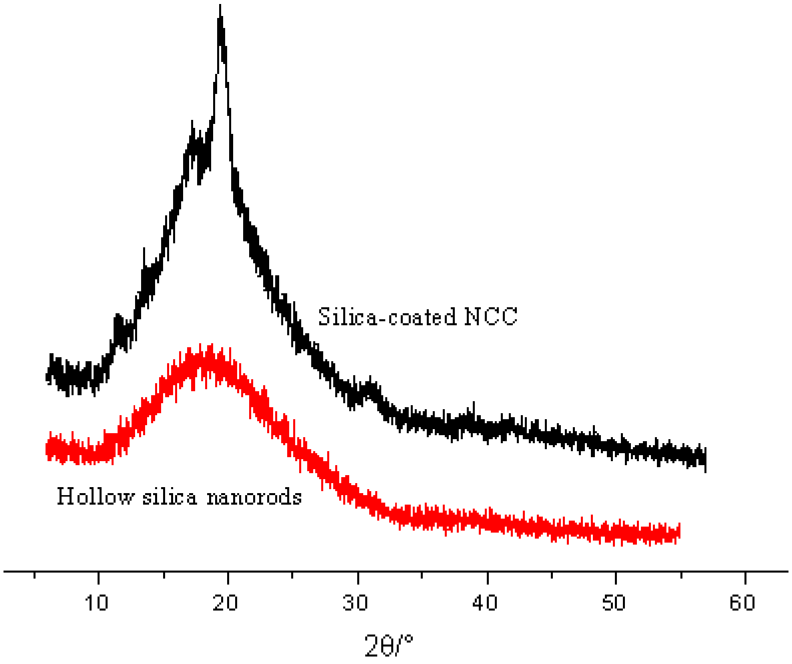

Fig. 5. XRD of silica-coated nanocrystalline cellulose and hollow silica nanorods

XRD results for silica-coated nanocrystalline cellulose and hollow silica nanorods are presented in Fig. 5. From comparison, the silica-coated nanocrystalline cellulose has smaller peaks at 16°, 22°, and 33°; these are the characteristic peaks of cellulose, as presented in Fig. 1(c). Because the proportion of cellulose is very small, one can see that the curve mainly corresponded to that of silica. Hollow silica nanorods exhibited a broad peak near 20°, the same peak as silica reported in the literature.

BET was employed to characterize the obtained silica-coated NCC and hollow silica nanorods. The specific surface area of silica-coated NCC was only 36.4 m^2/g, while after calcination it increased up to 1499.7 m^2/g. One can see that the specific surface area of hollow silica nanorods was much greater than silica-coated NCC. The increment of specific surface area was caused not only by the exposure of interior surface of nanorod tubes, but also caused by the addition of CTAB, which renders the wall of nanotubes mesoporous (Le *et al.* 2007). So, hollow nanorods obtained in our experiment gave rise to a large surface area, indicating that the produced hollow silica nanorods can be suitable for a number of promising applications.

CONCLUSIONS

1. A simple approach is reported for the fabrication of hollow silica nanorods using nanocrystalline cellulose (NCC) as templates, taking advantage of negatively charged nanocellulose crystals prepared by sulfuric acid hydrolysis.
2. The obtained hollow silica nanorods have uniform shape with the length of *ca*. 100 to 150 nm, inner diameter of *ca*.10 nm, and the thickness of 10 to 15 nm. The hollow silica nanorods are mesoporous, and the specific surface area can reach up to around 1500 m^2/g.
3. The results show that NCC is an ideal template for manufacturing nano hollow materials with uniform shape and size.

ACKNOWLEDGMENTS

The authors are grateful for the support of Research Fund for the Doctoral Program of Higher Education of China (Grant No. 20103204120005), Talents Foundation of Nanjing Forestry University (163105003), and the Priority Academic Program Development of Jiangsu Higher Education Institutions.

REFERENCES CITED

Beck-Candanedo, S., Roman, M., and Gray, D. G. (2005). "Effect of reaction conditions on the properties and behavior of wood cellulose nanocrystal suspensions," *Biomacromolecules* 6(2), 1048-1054.

Bondeson, D., Mathew, A., and Oksman, K. (2006). "Optimization of the isolation of nanocrystals from microcrystalline cellulose by acid hydrolysis," *Cellulose* 13(2), 171-180.

Caruso, F. (2001). "Nanoengineering of particle surfaces," *Adv. Mater.* 13(1), 11-22.

Caruso, F., Caruso, R. A., and Mohwald, H. (1998). "Nanoengineering of inorganic and hybrid hollow spheres by colloidal templating," *Science* 282(5391), 1111-1114.

Chen, J.-F., Ding, H.-M., Wang, J. X., and Shao, L. (2004). "Preparation and characterization of porous hollow silica nanoparticles for drug delivery application," *Biomaterials* 25(4), 723-727.

China National Pulp and Paper Research Institute and Beijing Chemical Plant (1981). "Cellulose crystallinity checked by infra-red spectrography-I: its procedues and relationship with crystallinity index checked by XRD and relationship with beating degree," *China Pulp Paper* (3), 11-20.

Guo, D.-J., and Cui, S.-K. (2009). "Hollow PtCo nanospheres supported on multi-walled carbon nanotubes for methanol electrooxidation," *J. Colloid Interface Sci.* 340(1), 53-57.

Kato, N., Ishii, T., and Koumoto, S. (2010). "Synthesis of monodisperse mesoporous silica hollow microcapsules and their release of loaded materials," *Langmuir* 26(17), 14334-14344.

Kim, J., Montero, G., Habibi, Y., Hinestroza, J. P., Genzer, J., Argyropoulos, D. S., and Rojas, O. J. (2009). "Dispersion of cellulose crystallites by nonionic surfactants in a hydrophobic polymer matrix," *Polym. Eng. Sci.* 49(10), 2054-2061.

Le, Y., Pu, M., and Chen, J.-F. (2007). "Theoretical and experimental studies on the silica hollow spheres," *J. Non-Cryst. Solids* 353(2), 164-169.

Lucia, L. A., Habibi, Y., and Rojas, O. J. (2010). "Cellulose nanocrystals: Chemistry, self-assembly, and applications," *Chem. Rev.* 110(6), 3479-3500.

Lucia, L. A., and Hubbe, M. A. (2008). "Book review: '*Materials, Chemicals & Energy from Forest Biomass*'," *Bioresources* 3(3), 668-669.

Lucia, L. A., and Rojas, O. J. (2009). *The Nanoscience and Technology of Renewable Biomaterials*, Wiley Online Library.

Min, B. G., Bae, G. Y., Jeong, Y. G., Lee, S. C., Jang, J. H., and Koo, G. H. (2009). "Superhydrophobicity of cotton fabrics treated with silica nanoparticles and water-repellent agent," *J. Colloid Interface Sci.* 337(1), 170-175.

Morán, J., Alvarez, V., Cyras, V., and Vázquez, A. (2008). "Extraction of cellulose and preparation of nanocellulose from sisal fibers," *Cellulose* 15(1), 149-159.

Nelson, M., and O'Connor, R. (1964a). "Relation of certain infrared bands to cellulose crystallinity and crystal latticed type. Part I. Spectra of lattice types I, II, III and of amorphous cellulose," *J. Appl. Polym. Sci.* 8(3), 1311-1324.

Nelson, M. L., and O'Connor, R. T. (1964b). "Relation of certain infrared bands to cellulose crystallinity and crystal latticed type. Part II. Spectra of lattice types I, II, III and of amorphous cellulose," *J. Appl. Polym. Sci.* 8(3), 1325-1341.

Obare, S. O., Jana, N. R., and Murphy, C. J. (2001). "Preparation of polystyrene-and silica-coated gold nanorods and their use as templates for the synthesis of hollow nanotubes," *Nano Letters* 1(11), 601-603.

Pei, A., Malho, J. M., Ruokolainen, J., Zhou, Q., and Berglund, L. A. (2011). "Strong nanocomposite reinforcement effects in polyurethane elastomer with low volume fraction of cellulose nanocrystals," *Macromolecules* 44(11), 4422-4427.
Ras, R. H. A., Kemell, M., de Wit, J., Ritala, M., ten Brinke, G., Leskelä, M., and Ikkala, O. (2007). "Hollow inorganic nanospheres and nanotubes with tunable wall thicknesses by atomic layer deposition on self-assembled polymeric templates," *Adv. Mater.* 19(1), 102-106.
Ras, R. H. A., Ruotsalainen, T., Laurikainen, K., Linder, M. B., and Ikkala, O. (2007). "Hollow nanoparticle nanotubes with a nanoscale brick wall structure of clay mineral platelets," *Chem. Commun.*(13), 1366-1368.
Scheel, H., Zollfrank, C., and Greil, P. (2009). "Luminescent silica nanotubes and nanowires: Preparation from cellulose whisker templates and investigation of irradiation-induced luminescence," *J. Mater. Res.* 24(05), 1709-1715.
Stöber, W., Fink, A., and Bohn, E. (1968). "Controlled growth of monodisperse silica spheres in the micron size range," *J. Colloid Interface Sci.* 26(1), 62-69.
Xiao, Q.-G., Tao, X., Zhang, J.-P., and Chen, J.-F. (2006). "Hollow silica nanotubes for immobilization of penicillin G acylase enzyme," *J. Mol. Catal. B: Enzym.* 42(1-2), 14-19.
Zhao, Y., Lin, L.-N., Lu, Y., Chen, S.-F., Dong, L., and Yu, S.-H. (2010). "Templating synthesis of preloaded doxorubicin in hollow mesoporous silica nanospheres for biomedical applications," *Adv. Mater.* 22(46), 5255-5259.
Zhou, C., Chu, R., Wu, R., and Wu, Q. (2011). "Electrospun polyethylene oxide/cellulose nanocrystal composite nanofibrous mats with homogeneous and heterogeneous microstructures," *Biomacromolecules* 12(7), 2617-2625.
Zollfrank, C., Scheel, H., and Greil, P. (2007). "Regioselectively ordered silica nanotubes by molecular templating," *Adv. Mater.* 19(7), 984-987.
Zoppe, J. O., Peresin, M. S., Habibi, Y., Venditti, R. A., and Rojas, O. J. (2009). "Reinforcing poly(epsilon-caprolactone) nanofibers with cellulose nanocrystals," *ACS Appl. Mater. Interfaces* 1(9), 1996-2004.

Article submitted: November 20, 2011; Peer review completed: January 8, 2012; Revised version received: March 29, 2012; Accepted: March 30, 2012; Published: April 10, 2012.